Biophysics

Volume 2, Issue 3, 284-302.
DOI: 10.3934/biophy.2015.3.284
Received date 07 May 2015,
Accepted date 02 July 2015,
Published date 30 July 2015

http://www.aimspress.com/

Research article

Effects of the Lipophilic Core of Polymer Nanoassemblies on Intracellular Delivery and Transfection of siRNA

Steven Rheiner [1], Piotr Rychahou [2,3], and Younsoo Bae [1,*]

[1] Department of Pharmaceutical Sciences, College of Pharmacy, University of Kentucky, 789 South Limestone, Lexington, KY 40536, USA
[2] Markey Cancer Center, University of Kentucky, 800 Rose Street, CC140, Lexington, KY 40536
[3] Department of Surgery, College of Medicine, University of Kentucky, 741 South Limestone, Lexington, KY 40536, USA

* **Correspondence:** Email: younsoo.bae@uky.edu; Tel: +1-859-323-6649; Fax: +1-859-257-7564.

Abstract: Despite effective gene silencing in vitro, in vivo delivery and transfection of siRNA remain challenging due to the lack of carriers that protect siRNA stably in the body. This study is focused to elucidate the correlation between complex stability and transfection efficiency of siRNA carriers. The carriers were prepared by using polymer nanoassemblies made of a cationic branched polymer [poly(ethylene imine): bPEI] to which hydrophilic poly(ethylene glycol) polymers were tethered covalently. These polymer tethered nanoassemblies (TNAs) were further modified with lipophilic chains (palmitate: PAL) in the core to stabilize siRNA TNAs complexes through ionic and hydrophobic interactions in combination. The effects of PAL in the core of TNAs were investigated with respect to in vitro transfection, intracellular gene delivery, and toxicity of the complexes, using a human colon cancer HT29 cell line stably expressing a luciferase reporter gene. A commercial transfection agent (RNAiMax) was used as a control. TNAs entrapping siRNA showed the greatest complex stability in the absence of PAL although TNAs with a greater PAL content induced effective intracellular siRNA delivery, while luciferase expression decreased as the amount of PAL increased in the core of TNAs. These results demonstrate that lipophilic components in carriers affect not only complex stability but also intracellular distribution and transfection of siRNA in cancer cells.

Keywords: polymer nanoassemblies; gene therapy; siRNA delivery; non-viral vectors; cancer; nanotechnology

1. Introduction

Gene therapy using siRNA has been investigated to treat various types of diseases, including cancer [1,2]. siRNA is a small, double-stranded RNA (19–23 base pair) that can attenuate the expression levels of complementary mRNA through degradation via the RNA interference pathway (RNAi) [3,4]. This allows for targeted inhibition of proteins with a known mRNA sequence, including those that have no drug inhibitor available. Although siRNA therapy has shown much promise in vitro to inhibit such undruggable proteins, in vivo delivery of siRNA to targeted sites in the body has been difficult because few methods are available to prevent rapid clearance and degradation of siRNA in the bloodstream [5,6]. Therefore, there has been a push to develop siRNA delivery carriers that overcome these hurdles.

Multiple types of carriers have been studied to chaperone siRNA to its site of action [5,7]. Carriers typically incorporate siRNA through ionic complexation between anionic siRNA and cationic moieties native to the carriers. In this regard, cationic polymers have become a material of interest for siRNA delivery because of their inclusion of a large number of positively charged moieties which allows ionic complexation with negatively charged siRNA to form complexes called polyplexes [8,9,10]. Branched poly(ethylene imine) (bPEI) is an example of such a cationic polymer [11]. The poly-amine compound bPEI contains primary, secondary, and tertiary amines which can be used in combination to complex with siRNA in a high efficiency [12], resulting in bPEI offering a highly charged, nanosized delivery carrier for siRNA. In comparison to other cationic polymers and linear PEI, bPEI often shows lower toxicity to cells [13]. However, bPEI siRNA polyplexes have not found much success in vivo due to their instability in the presence of negatively charged serum proteins and other anions in the bloodstream [14].

To increase polyplex stability, cationic polymers are often mixed in excess with the siRNA to form polyplexes. However, cationic polymers that fail to interact with siRNA (often called free polymers) are left separate from the polyplex and often cause various adverse effects [15]. For example, polyplexes can dissociate when competing anions are present to interact with free polymers and break up the polymer's interaction with siRNA [16]. While cationic moieties are essential to form polyplexes with siRNA, cationic polymers used in excess can also create a large positive surface charge detrimental to the polyplexes safety and stability [17,18]. High surface charge and free polymers are known to reduce the particles circulation time in vivo, cause cytotoxicity, decrease stability of the formulation, and fail to protect siRNA before delivery to target sites [19,20]. These all culminate in a lack of transfection efficiency and safety of the siRNA formulation but modifications to the existing polymers could help to return the lost efficacy.

Modification of the cationic polymer systems can address these unwanted aspects of formulation [21]. Cationic surface charge can be attenuated through modification of the polymer with [poly(ethylene glycol): PEG] [22]. The addition of PEG can shield the polyplexes from its environment, neutralizing its surface charge and increasing the circulation time of the polyplex [23]. Free polymer in formulation can be decreased by increasing the stability of the particle through addition of attractive forces between the polymers. Hydrophobic interaction has been shown to enhance particle stability by allowing each polymer chain to interact with each other as well as the siRNA [24,25,26]. Nucleic acid strands have shown to interact with hydrophobic groups once their anionic charge has been neutralized which would further stabilize the complex [27]. Additionally if siRNA dissociates from the complex, the particle can stay together based on the hydrophobic

interactions and reduce free polymer [28]. Alternatively, linking all free cationic polymer together, effectively forming a unimolecular system, will reduce free polymer in formulation because it would remove free polymer from the system all together. By modifying a single cationic polymer to covalently link with multiple other cationic polymers, PEG, and hydrophobic groups, a uniform particle would be created with no ability to dissociate its components from itself yet siRNA would be free to associate and disassociate. By reducing the free polymer and surface charge of the cationic polymer delivery vehicle, efficacy and stability should increase resulting in increased transfection efficiency.

Based on these backgrounds, we hypothesized that siRNA transfection efficiency and safety will improve by protecting siRNA in the core of a unimolecular cationic nanoassembly with improved complex stability. To test this, this study set out to create polymer nanoassemblies stabilized with a lipophilic core and examine the effects of complex stability on transfection efficiency, toxicity, and intracellular siRNA delivery. We synthesized the polymer nanoassemblies by tethering hydrophilic polymer chains, PEG, onto a single polymer backbone (branched PEI: bPEI) while modifying the core of the nanoassemblies with lipophilic pendant groups (palmitate: PAL).

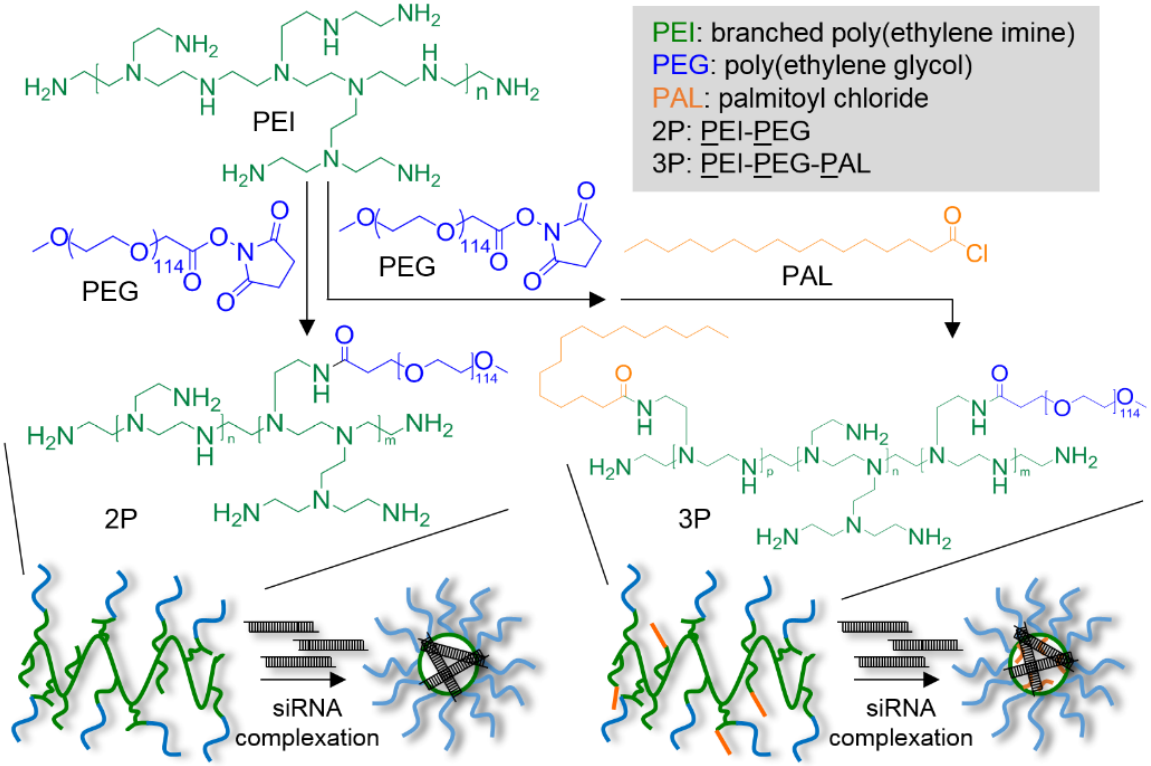

Figure 1. Synthesis of tethered nanoassemblies (TNAs) for siRNA delivery. TNAs were designed to form a unimolecular assembly entrapping siRNA in the core. The amount of PAL was controlled to modify lipophilicity of the core of TNAs.

Figure 1 illustrates two types of polymer tethered nanoassemblies (TNAs) used in this study, PEG-PEI (2P) and PEG-PEI-PAL (3P). 2P has cationic moieties in the core and thus attract siRNA to prepare polyionic complexes while 3P has a hydrophobic core modified with PAL to increase stability of the complexes through ionic and hydrophobic interactions between the core and siRNA

payload. The PAL content in 3P was also modulated at varying ratios to prepare TNAs that behave in between 2P and 3P. For this study, the siRNA-loaded TNAs were designed to reduce luciferase, an exogenous bioluminescent protein, expression level within a cell so that its efficacy in vitro could be examined through a facile method.

2. Materials and Method

2.1. Chemicals and cells

PEG (5 kDa, α-methoxy-ω-NHS activated) was purchased from NanoCS (New York, NY). Branched PEI (bPEI) and palmitoyl chloride were purchased from Sigma Aldrich (St. Louis, MO). HEPES buffer (pH 8.0, 1 M), pyridine, NuSieve agarose gtg, dialysis membrane with molecular cut-off (MWCO) of 8 and 100 kDa, dylight-547, Lysotracker, and other organic solvents were purchased from Fisher Scientific (Waltham, MA). siRNA was synthesized with a sequence of 5'-GUUGGCACCAGCAGCGCACUU-3', and a siGLO RISC-free control siRNA was purchased from GE Dharmacon (Lafayette, CO). A human colon cancer HT-29 cell line was purchased from American Type Culture Collection (ATCC, Manassas, VA). McCoy's 5A, 0.05% trypsin/EDTA, and phosphate buffered saline (PBS) were from GE Healthcare (Logan, UT). Fetal bovine serum (FBS) was purchased from Atlanta Biologicals (Flowery Branch, GA). HT-29 cells were cultured in McCoy's 5A media supplemented with 10% FBS according to all ATCC recommendations. Cells were maintained at logarithmic growth in a humidified environment with 5% CO_2 at 37 ℃.

2.2. Polymer tethered nanoassembly (TNA) synthesis

TNAs were synthesized from 25 kDa bPEI, 5 kDa NHS-PEG, and Palmitoyl chloride. Before use, bPEI was dialyzed using 100 kDa MWCO membrane against water for 1 day to remove small impurities. bPEI was reacted with 5 kDa PEG NHS ester, at a 1:100 molar ratio, in a mixed solution of DMSO and HEPES (1:1) at room temperature. The reaction produced PEG-PEI (2P), which was purified by dialysis using a 100 kDa MWCO membrane for 5 days in water, and collected by freeze drying. PEG-PEI was further reacted with palmitoyl chloride at 1:100, 1:50, and 1:30 molar ratios in THF at 40 ℃ for 2 hours in the presence of pyridine as a scavenger of a hydrochloric acid byproduct to create PEG-PEI-PAL (3P), 3P mid, and 3P low respectively. The reaction solutions were precipitated in diethyl ether and subsequently dialyzed in water prior to freeze drying.

2.3. Validation of TNA synthesis

The purity and uniformity of TNAs were determined by gel permeation chromatography (GPC) (Asahipak GF-7M column, 2 mg/mL, PBS, 0.5 mL/min, 40 ℃) Molecular weights were determined by comparing peak retention time to PEG standards. The diameter and surface charge of TNAs were determined by dynamic light scattering and zeta potential measurements (Zetasizer Nano, Malvern, UK). Particle solutions of 2 mg/ml were loaded into disposable zeta cuvettes and read for particle size and then zeta potential in the usage.

2.4. Fluorescamine assay for extent of palmitoylation

Extent of palmitoylation was examined by fluorescamine assay. Fluorescamine powder was dissolved in DMSO to 10 mg/ml. Particles were dissolved in a 50/50 mixture of DMSO/water to a concentration of 1 mg/ml. 100 μL of each particle solution and blank DMSO/water was added to a clear 96 well plate and then 10 μL of the fluorescamine solution was added immediately before reading on a fluorescent plate reader at 390/460 excitation/emission (SpectraMax M5, Molecular Devices). The fluorescence intensity of the blank was subtracted from the experimental wells and then experimental wells compared with each other.

2.5. Particle-siRNA complexation agarose gels

Complexes were formed by mixing solutions of particles at several concentrations from 0.1 and 100 mg/ml in Optimem with 720 nM siRNA in Optimem. Solutions were mixed at a 1:1 ratio and allowed to equilibrate for 30 minutes at room temperature. 20 μL of each solution and 5 μL of low range DNA ladder were loaded to 4% agarose gel and run at 100 volts for 80 minutes at room temperature. The gel was stained in 200 ml of 100 ng/ml ethidium bromide in TAE (Tris-Acetate 0.04 M, EDTA 0.001M) buffer, rinsed 3 times in TAE buffer, and imaged via Typhoon GLA 9500 (GE Healthcare, Logan, UT) fluorescent imager under the ethidium bromide filter set.

2.6. Particle-siRNA release study

Complexes were formed by mixing solutions of particles, concentrated in optimem media at 10 mg/ml, with 720 nM fluorescently-labeled siRNA optimem solution at a 1:1 ratio to a final concentration of 5 mg/ml of particle and 360 nM of siRNA for 30 minutes at room temperature. 20 μL of the complex solutions were added to 10 μL solutions of varying heparin concentration. 0, 10, 100, 1000, and 5000 μg/ml concentrations were used to create weight ratios of siRNA/heparin between 0 and 500. 10 minutes later, 20 μL of each solution was loaded onto an agarose gel and run at 100 V for 80 minutes. The gel was imaged using Typhoon equipped with a cy3 filter set (dylight-547 compatible).

2.7. siRNA protection study

Complexes prepared for particle-siRNA release study above were also used for siRNA protection study. Complex solutions (20 μL) were incubated with 20 μL of active FBS or heat-inactivated FBS. A control was created by adding complex solution to RNase free water (20 μL, respectively) and then frozen. 20 μL of sample solution was loaded and run on 4% agarose gel in TAE buffer at 100 V for 80 minutes. After the gel was run, the gel was imaged with Typhoon through the cy3 filter set.

2.8. In vitro transfection assay

Cells were seeded at 5,000 cells per well into a white opaque 96 well plate for 24 hours. After 24 hours, Complex solutions were created by mixing 100 μL of 10 mg/ml particle solutions with

100 μL of 720 nM anti-luciferase siRNA, all solution in optimem. These were incubated at room temp for 30 minutes. Control Solutions were created by setting aside 200 μL of optimem for a blank control and mixing 100 μL of 720 nM anti-luciferase siRNA solution with 100 μL optimem or 100 μL of optimem containing 5 μL of RNAiMAX agent to create a naked siRNA control and RNAiMAX control, respectively. These were incubated at room temp for 30 minutes except the RNAiMAX control which was incubated for 20 minutes, per manufacturer's instructions. 180 μL of each solution was added to 720 μL of McCoy's 5A supplemented with 10% FBS creating a final concentration of 1 mg/ml particle concentration, 72 nM siRNA, and 0.5 μL well of RNAiMAX concentration. Media was removed from each well and 100 μL of complex solutions and controls were added to the wells, n = 8. The plates were incubated until their endpoints (24, 48, or 72 hours) and then assayed for bioluminescence. Wells were injected with 100 μL of 0.1 mg/ml luciferin solution in PBS via a GloMax luminometer (Promega). Bioluminescence intensity was integrated over a 10 second period and recorded by the luminometer. Blank control wells were used to compare normal bioluminescence intensity to the experimental wells and data is reported as percentage luciferase activity. This data was then normalized based on a viability assay described later to account for cell death in the reduction of luciferase signal. For the 2P/3P combination experiments after 24 hours incubation, 20 μL of media was removed from each well. 20 μL of 10 mg/ml 3P optimem solution was added to wells containing 2P and 20 μL of optimem was added to all other wells. Cells were then incubated for a further 48 hours, and subjected to viability and bioluminescence assays as described previously.

2.9. In vitro toxicity assay

After the transfection assay was completed, each plate underwent a resazurin assay. 10 μL of a 1 mM solution of resazurin in PBS was added to each well of the 96 well plate. The plate was returned to the incubator for 3 hours and then read on a SpectraMax M5 (Molecular Devices) fluorescent plate reader at an excitation/emission of 560/590. A control of blank media with resazurin was used to subtract out background fluorescence and then fluorescence intensity was compared between each experimental well and the blank control wells to give a percentage of viable cells.

2.10. Intracellular siRNA imaging

Eight well glass slides were plated with 10,000 cells per well in McCoy's 5A media supplemented with 10% FBS. 24 hours later, complex solutions were created based on the endpoint of the imaging study. To image siRNA within the cell, 30 μL of 10 mg/ml unlabeled particle solutions with 30 μL of 720 nM dylight-547 labeled siRNA were mixed. To image siRNA/particle colocalization, 30 μL of 10 mg/ml fluorescein labeled particle solutions with 30 μL of 720 nM dylight-547 labeled siRNA were mixed. To image particle/lysosome colocalization, 30 μL of 10 mg/ml fluorescein labeled particle solutions with 30 μL of 720 nM unlabeled siRNA were mixed. To image combination of 2P/3P, 30 μL of 10 mg/ml fluorescein labeled 2P solutions with 30 μL of 720 nM unlabeled siRNA were mixed. Controls of naked siRNA and blanks were created by mixing 30 μL of 720 nM dylight-547 labeled siRNA with 30 μL of optimem and 30 μL of optimem with 30 μL of optimem, respectively. All solutions were incubated at room temp for 30 minutes. Afterwards, 60 μL of each solution was added to 240 μL of McCoy's 5A supplemented with 10%

FBS creating a final concentration of 1 mg/ml particle concentration and 72 nM siRNA. Media was then removed from each well and 200 μL of complex solutions were added to the wells and incubated for 48 hours. Additionally for the 2P/3P combination study, 24 hours after dosage 30 μL of media was removed from the well and 30 μL of 10 mg/ml fluorescein labeled 3P was added. 48 hours after dosage, cells were rinsed with PBS 3 times, fixed with formalin for 20 minutes, stained with Hoechst 33342 and Lysotracker red (if applicable), and rinsed another 3 times. Cells were imaged at 100X on a Zeiss axiovert 200M fluorescent microscope using dapi, texas red, and fluorescein filter sets. Images were captured with the fluorescein and Texas Red filters for fluorescein particles and siRNA, respectively, while using the same exposure between images to compare fluorescent intensity between them.

2.11. Particle uptake pathway study

Cells (5,000 cells/well) were seeded into a white 96 well plate. After 24 hours, complex solutions and controls were created by mixing 100 μL of 720 nM dylight-547 labeled siRNA optimem solution with 100 μL of 10 mg/ml 3P optimem solution or 100 μL of optimem, respectively. These were incubated at room temp for 30 minutes. One plate was stored in 4C for 30 minutes along with particle and control solutions to be used with the plate. Media was removed from the wells and 100 μL of control and complex solutions were added to the plate (n = 4). The plate was returned to 4 ℃. Another plate was treated identically but kept at 37 ℃. After 4 hours, the plates were rinsed with cold PBS three times and read on a fluorescent plate reader at excitation/emission of 557/570. The fluorescence intensity was compared with an untreated control well at each temperature.

3. Results

3.1. TNA Synthesis

TNAs were synthesized as shown in Figure 1. All TNAs were uniform and contained no impurities as confirmed by a single peak shown on GPC (Figure 2). DLS and zeta-potential measurements confirmed that 2P and 3P were less than 40 nm in diameter and had a neutral surface charge regardless of PAL modification (Table 1). These results indicate that PAL is mostly present in the core of TNAs and the PEG shell efficiently shields the charge and hydrophobic groups. However, there is a discrepancy between the DLS measured polydispersity index (PDI) and the sharpness of the GPC peak from 3P.

Modification of the core with PAL groups did not seem to affect the surface properties of TNAs although it altered lipophilicity and molecular conformation of the core. GPC revealed that the molecular weights of 2P and 3P were 128 and 158 kDa, respectively. Although the exact number of primary amines on bPEI is unknown, our estimation based on the molecular weights of bPEI (25 kDa) and TNAs suggests that approximately 10% and 55% of binding sites on bPEI were conjugated with PEG and PAL, respectively. To further confirm the reaction, a fluorescamine assay was used to compare the amounts of remaining primary amines between 2P and 3P. 3P contained fewer primary amines per particle than 2P, corresponding with the GPC estimation.

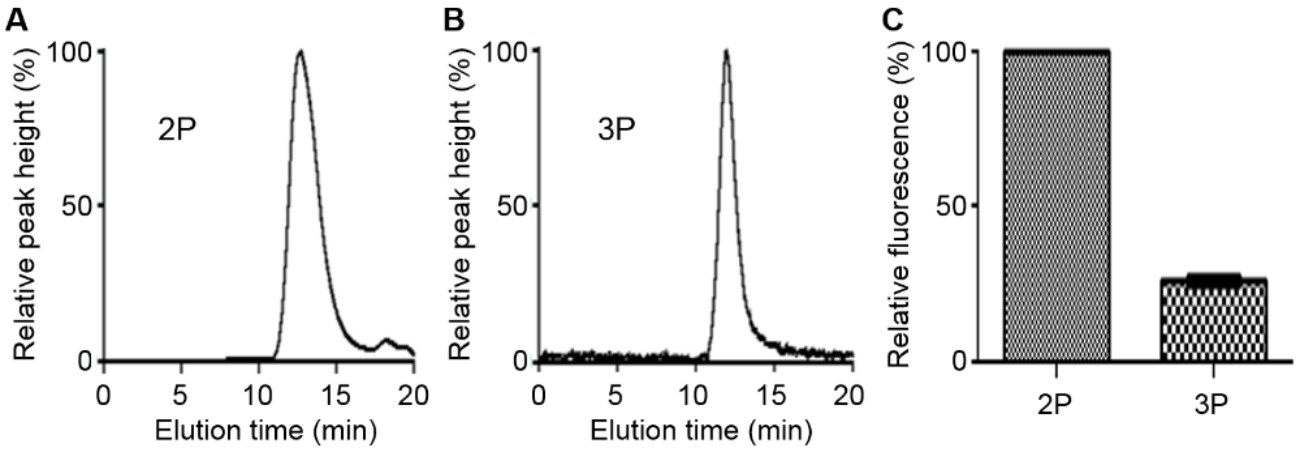

Figure 2. Characterization of TNAs. GPC spectra showing uniform distributions of 2P (A) and 3P (B). Fluorescamine assay results (C) for quantification of primary amines remaining in the core of TNAs.

Table 1. Particle diameter, polydispersity index, and zeta potential of 2P and 3P particles.

	2P	3P
Size (nm)	23.19 ± 1.05	34.33 ± 3.95
PDI	0.18	0.559
Zeta Potential (mV)	2.66 ± 0.32	−1.99 ± 0.23

3.2. Characterization of TNA's interactions with siRNA

Interactions between siRNA and TNAs were characterized in 3 different ways: siRNA uptake by TNAs, binding strength of TNA to siRNA, and protection of siRNA from degradation. To confirm siRNA entrapment, Figure 3 shows various concentrations of particle complexed with a constant amount, 5 μg/ml for effective visualization, of siRNA. 2P showed partial siRNA entrapment at particle concentrations between 0.05 and 0.5 mg/ml, and full complexation at 5 mg/mL and above. This gives the weight ratio between particle and siRNA necessary for complete entrapment of siRNA within the particle. 3P showed partial entrapment only at 50 mg/ml yet required a concentration for complexation too high for in vitro experiments.

Figure 3 also shows how strongly siRNA was bound to the particles by measuring its release from siRNA TNA complexes after incubation with increasing anion/siRNA weight rations of a competing anion heparin, a glycosaminoglycan found in extracellular matrices of many tissues. This was used to mimic conditions the TNA complex would encounter once inside the cell as ionic binding competition is the most common method of siRNA release. 2P appeared to require a large ratio of heparin to release siRNA, indicating a large binding affinity, while 3P showed no heparin necessary for release as it failed to form stable complexes with siRNA.

In order to examine the potential of TNAs to protect siRNA from degradation, TNA complexes were incubated with a high level (50%) of FBS. Both naked siRNA and 3P complexes were unstable in the presence of both active and heat-treated FBS due to nuclease degradation, whereas 2P

protected siRNA for the duration. This was expected as 3P had not previously shown complexation with siRNA but 2P had shown tight binding to the siRNA. These results would give 2P greater potential as an in vivo formulation compared with 3P because of 2Ps ability to form complexes and protect the siRNA.

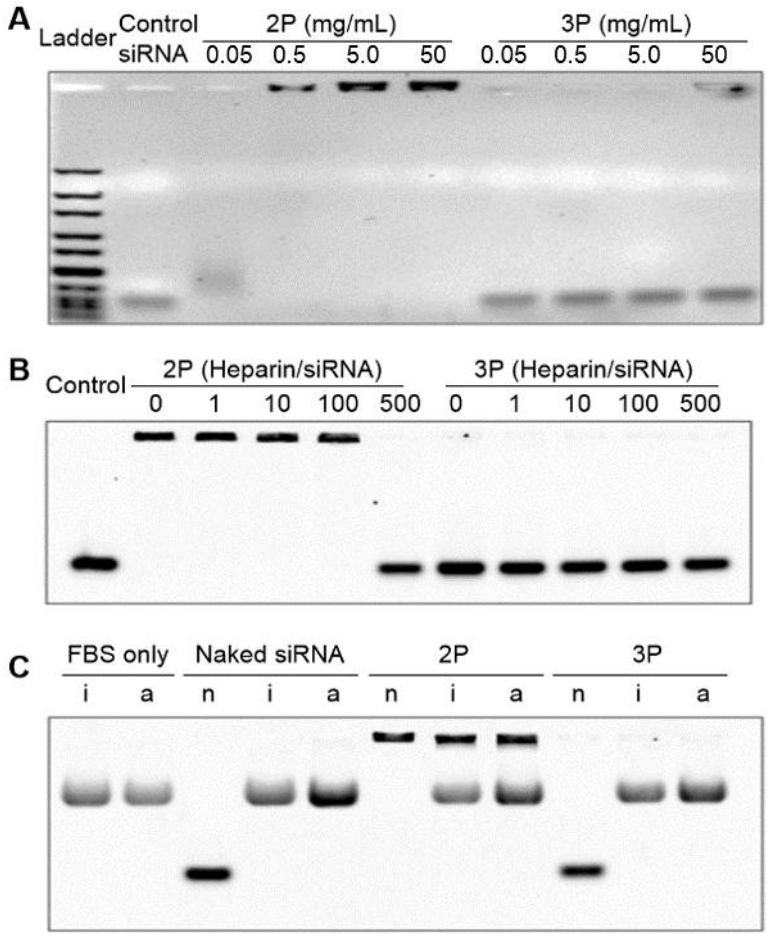

Figure 3. Complex formation and stability of TNAs. TNAs were mixed with siRNA (360 nM) at varying ratios to determine a particle concentration required for forming neutral siRNA complexes (A). siRNA-loaded TNAs (5 mg/mL) were incubated with heparin to determine complex stability in the presence of anionic counterparts other than siRNA in a solution (B). siRNA-loaded TNAs were also incubated with nuclease free water (n), heat-inactivated FBS (i), and active FBS (a) to determine protective effects of TNAs in cell culture media with digestive enzymes (C). Naked siRNA at 360 nM and FBS alone used as controls.

3.3. Effect of TNAs on siRNA Transfection and Toxicity in vitro

In order to assess the delivery efficacy of the TNA complexes, bioluminescence was used as a facile method of protein reduction quantification. Luciferase protein was introduced to HT-29 colorectal adenocarcinoma cells so that it was stably expressed at all times (HT-29-LUC). Anti-luciferase siRNA uses the RNAi pathway to degrade luciferase mRNA, attenuating protein

production. This allows for easy detection of remaining protein by addition of luciferin substrate. The amount of protein remaining correlates to siRNA delivery efficacy [29].

HT-29-LUC cells were incubated with siRNA-TNA complexes and 72 hours later the cells were examined for luminescence and cell viability (Figure 4). Particle concentrations used were 1 mg/ml or 20% that of what was found to be full complexation in previous experiments (5 mg/ml) due to 20% the amount of siRNA (1 μg/ml) to be used in vitro. Initially, 2P showed no transfection but 3P showed approximately 70% reduction of the luciferase activity, attributed to siRNA delivery. The transfection efficiency of 3P was comparable to that of Lipofectamine RNAiMax, a commercially available transfection reagent. To further examine the transfection efficiency of both particles, transfection was monitored daily for total 4 days past dosage. 3P and RNAiMax showed a similar transfection profile, reducing luciferase expression continuously for 4 days, but 2P induced no transfection in the same period of time. Additionally, neither 2P nor 3P exhibited any noticeable toxicity under our experimental condition while RNAiMAX showed mild toxicity with approximately 20% reduction in cell viability.

Further confirmation of siRNA delivery was shown by fluorescent imaging with fluorescently labeled siRNA. This allowed for viewing of the amount of siRNA used within the cells for each formulation (Figure 5). Compared with the non-treatment and free siRNA incubated cells, both TNA formulations showed siRNA within the cell. However, cells incubated with 3P complexes showed a much larger fluorescent intensity through confocal microscopy than those incubated with 2P indicating that 3P was able to increase the amount of siRNA that would be trafficked into the cell.

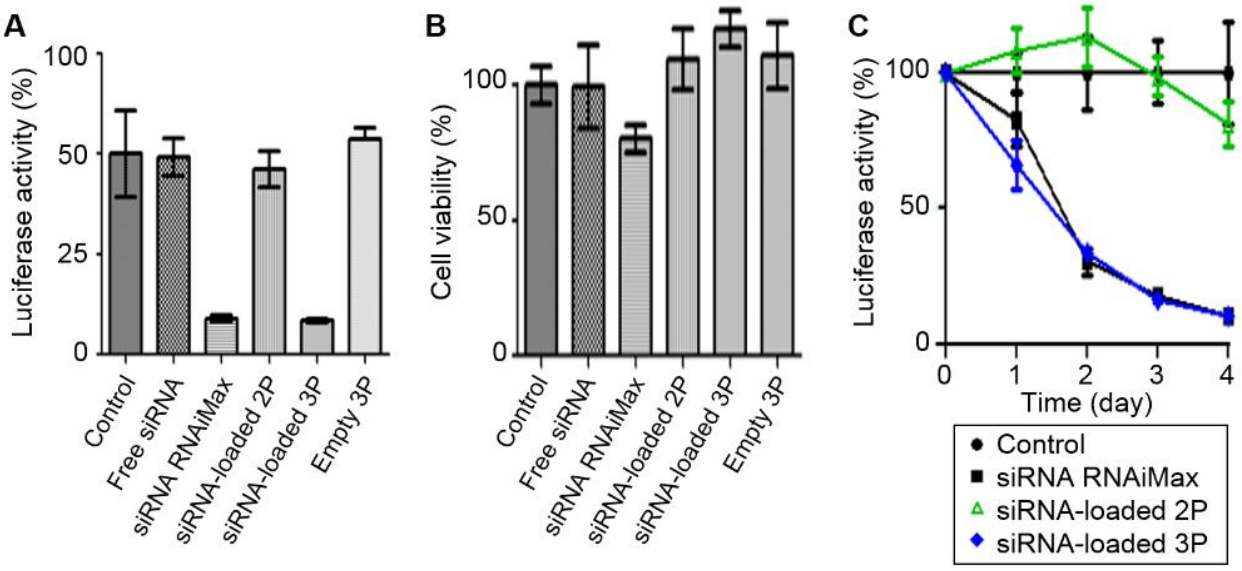

Figure 4. Transfection efficiency and toxicity of TNAs. A human colon cancer HT-29 cell line stably expressing a luciferase reporter gene was transfected with TNAs to monitor luciferase activity (A) and cell viability (B) after 72 hours of incubation. Transfection profiles over a 4 day period were taken to determine long-term gene silencing effects of TNAs (C).

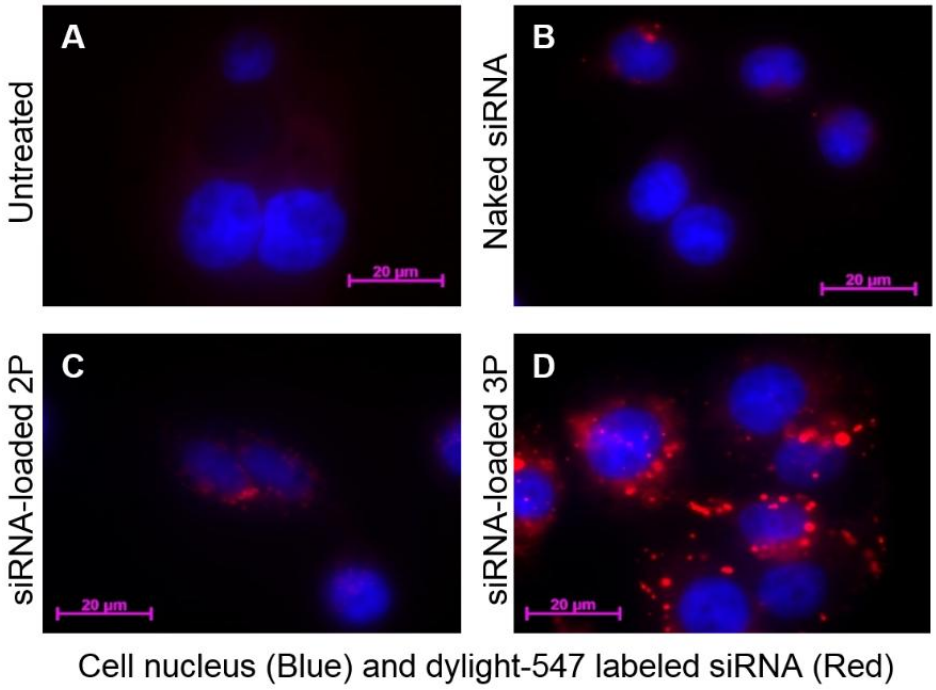

Figure 5. Fluorescent microscopy. HT29 cells were incubated with TNAs (1 mg/mL) containing dylight-547 labeled siRNA (72 nM) to confirm intracellular delivery of siRNA at 48 hours post-transfection, following the treatment of cells with PBS (A), naked siRNA (B), 2P complexes (C), and 3P complexes (D).

3.4. Intracellular siRNA trafficking

Because of PAL's ability to interact with cellular membranes, it was necessary to determine if the 3P particle was entering the cell through an endocytotic pathway or through membrane disruption (Figure 6). To observe this, cells were incubated with TNA complexes containing fluorescent siRNA at 4 ℃ and 37 ℃. At 4 ℃ endocytosis is significantly reduced whereas at 37 ℃ cells operate under normal conditions. By comparing intracellular uptake of TNAs at these temperatures the importance of an endocytotic pathway in TNA uptake can be elucidated. The results show larger fluorescent intensity for those cells incubated at 37 ℃, indicating that TNAs enter the cell through endocytosis in a greater amount than non-specific membrane disruption as seen with other cationic polymers and PAL-conjugated bPEI.

Intracellular fluorescent imaging was further used to elucidate TNA complex intracellular distribution and siRNA release, following cell internalization (Figure 7). First, siRNA release from the TNAs was examined. Fluorescein labeled TNA complexes with dylight-547 labeled siRNA were incubated with cells for 48 hours. 2P was colocalized greatly with siRNA which would result in minimal siRNA being released into the cells. Minimal siRNA release would result in low or no transfection occurring and this correlates well with the previous in vitro results. 3P showed little colocalization, as would be expected with its lack of complex formation.

Next, endosomal escape by the TNA complexes was examined. Fluorescein labeled TNA complexes were incubated with cells similarly and dyed with a lysosome stain. 2P complexes colocalized in lysosomes and 3P complexes showed less lysosomal colocalization. These results

suggest 2P did not escape endosomes as efficiently as 3P and 2P's reduced transfection efficiency was attributed to less endosomal escape.

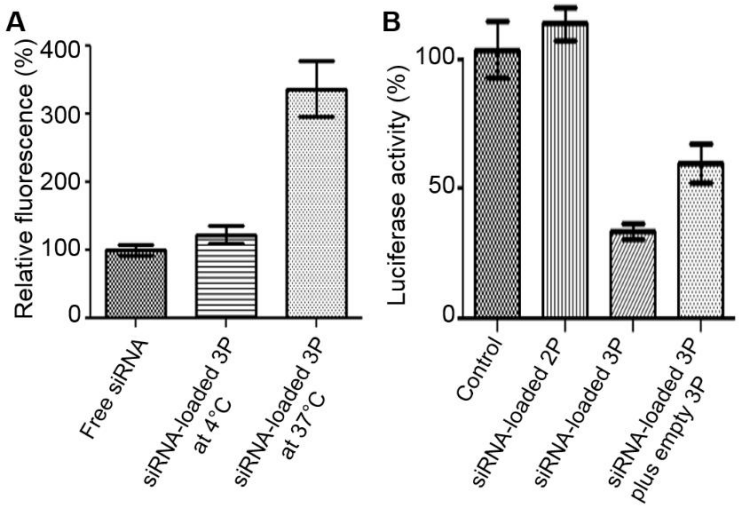

Figure 6. Elucidation of siRNA transfection mechanisms for TNAs. Cells were treated with siRNA-loaded TNAs at an incubation temperature that endocytosis is active (37 ℃) or suppressed (4 ℃) to determine the intracellular uptake mechanism for TNAs (A). Cancer cells treated with siRNA-loaded 2P were incubated with empty 3P at 24 hours post transfection to demonstrate a unique property of 3P that enhances siRNA transfection alone or in combination with 2P (B).

3.5. 2P-3P Combination Dosage

A combinatorial approach to TNA transfection was examined to help elucidate 3P's role in transfection efficacy as well as attempt to protect siRNA while achieving transfection. 2P-siRNA complexes were incubated with cells for 24 hours and then empty 3P particles introduced (Figure 6). It was found that the addition of empty 3P did increase the transfection efficiency of 2P-siRNA complexes from 0% to 60%.

A closer look at the intracellular trafficking of this dosage was achieved through fluorescent microscopy. Decreased colocalization seemed to occur between siRNA and particle compared with 2P as shown in Figure 7. Figure 7 also showed less colocalization between endosome and particle, indicating that particles and siRNA were escaping endosomes, previously not seen with 2P particles alone. This gave a greater indication that 3P has a greater endosomal escape capability compared with 2P and that it may lend it to other particles taken up by the cell concurrently.

3.6. Variation of Palmitoylation of 3P

Because of the success of the 2P/3P combination approach, the ratio of PAL substitution on 3P was examined to find an optimal ratio where 3P could form complexes with siRNA. This would enable 3P to protect cells so that a less complicated approach could be taken compared to the combination 2P/3P described in the previous section. Two additional TNAs were synthesized by

aiming for 15% and 25% palmitoylation of 2P, named 3P low and 3P mid, respectively. The amounts of primary amines remaining in the core of 3P low and 3P mid were determined by a fluorescamine assay (Figure 8). The assay indicated that palmitoylation was achieved at differing levels compared with the initial 3P particle. Gel electrophoresis was performed to confirm siRNA complexation with 3P low and 3P mid. 3P low achieved complexation between 0.5 mg/ml and 1.0 mg/ml, significantly lower than the original 3P at 72 nM siRNA concentration. 3P mid began to form partial complexes at 1 mg/ml but required a higher polymer concentration for complete complexation.

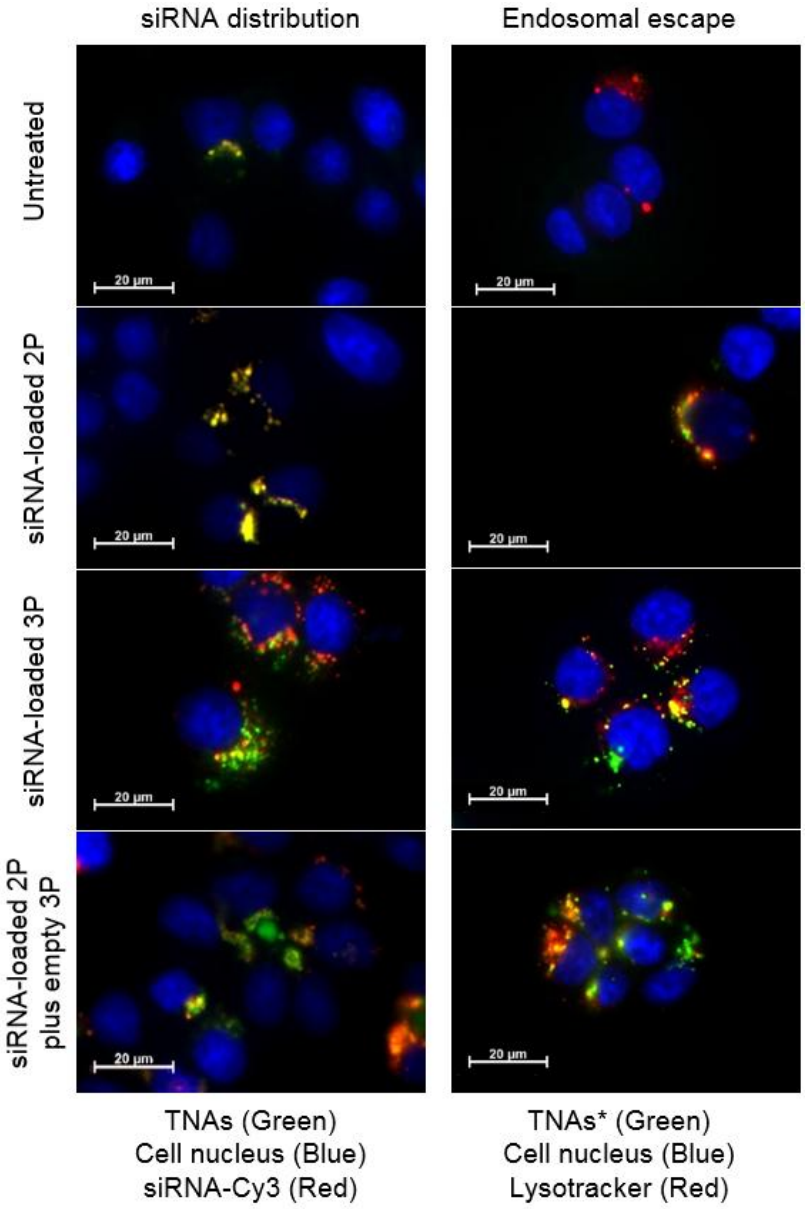

Figure 7. Intracellular distributions of siRNA-loaded TNAs. Fluorescence images of cells were taken at 48 hours post-transfection to determine the release of siRNA from TNAs as well as endosomal escape of TNAs during transfection. *TNAs were entrapped with non-labeled, anti-luciferase siRNA to avoid fluorescence signal interference between the siRNA and Lysotracker.

To examine the effect of palmitoylation on transfection efficiency, cells were incubated with each form of 3P complexes with siRNA for 72 hours. Though 3P low was able to maintain a complex with siRNA, it did not find more than 20% transfection efficiency but the partial complexes formed by 3P mid increased transfection efficiency further. This showed a positive correlation between PAL content on 3P and transfection efficiency as well as provided insight into PAL's role on transfection.

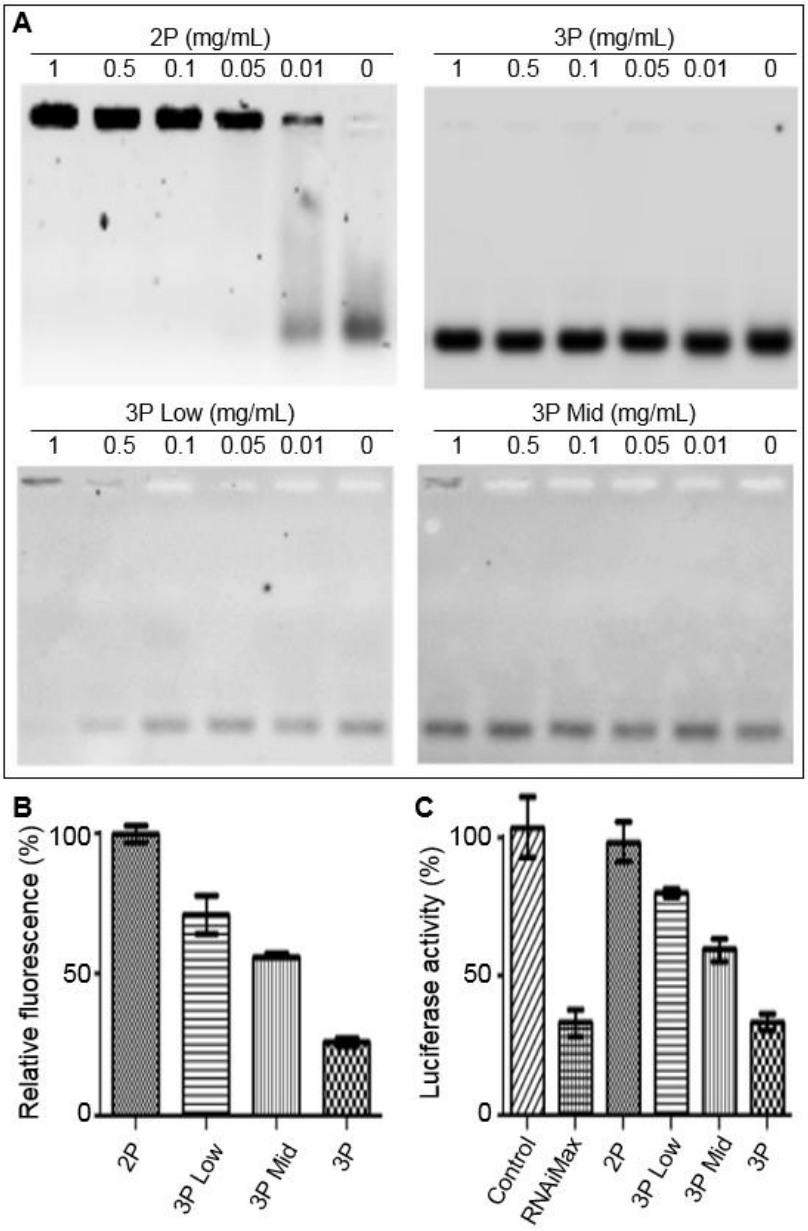

Figure 8. Complex formation and siRNA transfection of TNAs with varying PAL contents in the core. TNAs were confirmed to entrap siRNA less efficiently as the amount of PAL conjugated in the core increased, which were determined by gel electrophoresis (A) and fluorescamine assay (B), respectively. Conversely, siRNA-loaded TNAs transfected cells more efficiently during a 72 hour period as the amount of PAL in the core increased (C).

4. Discussion

Cancer therapy using siRNA has shown much promise at the in vitro level by reducing expression levels of undruggable proteins. However, very few of the formulations seen in vitro have moved on the in vivo level or the clinic. Most of the issues encountered in moving to in vivo involve toxicity and lack of stability in the bloodstream which ultimately lead to low transfection efficiency. Many formulations have attempted to address these issues by using a linked, or crosslinked [30,31], polymer system or a hydrophobic core [32] to stabilize the particle and complex. Here we have taken a linked system and introduced a hydrophobic core to examine its effects on stability and transfection efficiency as well as elucidate its effect on improving the system as a siRNA delivery vehicle.

In order for a delivery vehicle to be successful it must be able to do 3 things: deliver the siRNA to its target site, protect siRNA from degradation, and release the siRNA into the cytoplasm of the cell. Both physical properties of the particle and thermodynamic properties of the particle-siRNA complex can determine if it will meet these criteria and have a better chance at becoming an in vivo system [33]. In terms of physiochemical properties, both particles have beneficial surface charge and size for in vivo delivery. Each particle was pegylated, shown a neutral surface charge, and found to be between 20–40 nm in diameter which is beneficial for enhanced circulation time, decreasing off-target interactions [33,34].

While both particles had beneficial physical properties, only 2P was able to form a stable complex with siRNA. 2P was shown to bind strongly to siRNA and protect it from degradation. This tight binding, as seen by resistance to competing anions, would generally indicate an effective particle [35]. Resistance to competing anions is generally beneficial for siRNA complexes to avoid uncontrolled release of the genetic cargo in the bloodstream [16] but it is troubling from a therapeutic perspective if the complexes are too stable to release siRNA inside targeted cells [36]. In contrast, 3P was unable to form complexes at concentrations lower than 50 mg/ml or protect siRNA from degradation. This result was surprising because the fluorescamine assay indicated that 3P had primary amines available for complexation with siRNA but it required more than 100 times the amount of particle to show even slight complexation. The ratio of active amines to siRNA for complexation differed between 2P and 3P, indicating that the addition of PAL to the nanoparticle core can interfere with free primary amines possibly by condensing in the core around active amines to block their interaction with siRNA.

The result contradicted our initial hypothesis as PAL was expected to increase stability of the polyplex rather than reduce it. Though the primary amines may be hidden by the hydrophobic group, it may not affect fluorescamine interaction since the hydrophobic nature of fluorescamine and presence of organic solvent may allow for fluorescamine to interact. It is unclear if the addition of organic solvent during siRNA complexation would allow stable complex formation with 3P. Despite its lack of complex formation, 3P was able to transfect cells with much greater efficiency than 2P. Again, this would seemingly contradict traditional thinking that a strong complex is necessary for effective transfection. This must mean that 3P is moving siRNA into the cell differently than 2P, as we see a greater amount of siRNA within the cell after dosages. Particles enter cells in 2 main ways: endosomal pathway and membrane disruption [37]. Membrane disruption occurs when a lipid fuses with a membrane to create holes or help push particles through them. This has been seen with other lipid containing nanoparticles, such as liposomes and micelles [38,39]. Our particle design is expected to contain the lipid portion, PAL, within the core and it would be unable to interact with a

membrane, and therefore an endosomal pathway is more likely. After experimentation, it was found that endocytosis was the major pathway of particle uptake (Figure 6).

Knowing that the particle enters the cell in this manner, endosomal escape was the next ability to consider. Endosomal escape is the ability of a nanoparticle to remove itself from the endosome and enter the cytoplasm. While there are many mechanisms for this, bPEI exhibits the proton sponge effect [40]. The proton sponge effect is a type of hydrogen ion buffering where the hydrogen ions entering the endosome are absorbed by the amines within bPEI. This causes more and more chloride ions, which enter the endosome concurrently with hydrogen ions, to be pumped in the endosome in order to lower the pH, to become a lysosome. Eventually the endosome swells and bursts, releasing the particle [41]. This is considered to be the main mechanism of endosomal escape for many cationic polymer systems [42,43]. Another mechanism is cellular membrane disruption through direct interaction between cationic bPEI and anionic lipid layers [36], similar to cellular uptake by this mechanism. In this case the mechanism of endosomal escape is unclear but PAL addition seemed to be key in assisting disruption of the endosome. The colocalization images (Figure 7) showed that 2P was within the lysosomes with its siRNA payload but 3P had little colocalization with either. This mean that 2P has lost some of its natural endosomal escape property but addition of PAL to 3P returned an endosomal escape method, either by proton sponge or membrane disruption via PAL. This would show that PAL must play a major role in the 3P's transfection ability possibly through endosomal escape enhancement. However, it is important to note that based on design PAL is presumed to be within the core of 3P but the discrepancy between the PDI value and GPC peak could indicate some weak hydrophobic interaction between particles. Aggregates between small numbers of particles would account for large PDI seen via DLS measurement (table 1) and indicate a mild interaction with PAL between particles. This would not necessarily be seen in the GPC data due to shear stress and column interaction during measurement. Therefore, palmitate may be present in low amounts near the surface of the nanoparticle. Further study of how 3P delivered siRNA into the cell is necessary.

It must be noted that combination of beneficial aspects of 2P and 3P would provide an effective siRNA delivery system either by dosing a combination of 2P and 3P. Combination dosage was found to be successful in this study as 2P protected the siRNA from degradation while 3P enhances endosomal escape. Colocalization images backed this up, showing less particles within the endosome and less siRNA within the particles. This also shows that 2P is able to release its siRNA once it is within the cytoplasm of the cell. However, the success of this 'combined' formulation may depend on the co-delivery efficiency of both particles, and therefore developing a single particle system might be still a viable option. In this study, we have found that increasing lipophilicity of the core of siRNA TNA complexes with PAL would be beneficial to enhance siRNA transfection, as others have seen. However, PAL's hindrance to siRNA loading still remains a major challenge to developing polymer nanoassemblies with a lipophilic core for future clinical applications. It may be possible to optimize transfection efficiency and siRNA loading in polymer nanoassemblies by utilizing alternate moieties as the effect of the hydrophobic group in enhancing siRNA transfection appeared evident.

5. Conclusion

In this study, polymer nanoassemblies were used to evaluate the effects of lipophilicity of the nanoassembly core on biological outcomes such as intracellular delivery and transfection of siRNA.

Our results showed that nanoassemblies with a hydrophilic, cationic core (2P) are bound to siRNA too tightly to transfect the cells although the tight complexation was beneficial to protecting siRNA from degradation. On the other hand, nanoassemblies with a hydrophobic, partially cationic core (3P) appeared to fail to form stable siRNA complexes but enhance target gene silencing presumably due to enhanced intracellular uptake and endosomal escape of siRNA. Further investigation demonstrated that a combined formulation of 2P and 3P was effective to protect siRNA and achieve effective transfection, which revealed that PAL conjugated in the core of nanoassemblies played an important role in determining the fate of siRNA-loaded nanoassemblies in the cell. Taken together, we conclude from this study that ionic and hydrophobic interactions should be considered concurrently in the design of siRNA delivery carriers to guarantee stability and transfection efficiency.

Acknowledgments

This work is partially supported by the University of Kentucky Markey Cancer Center pilot project grant.

Conflict of Interest

All authors declare no conflicts of interest in this paper.

References

1. Resnier P, Montier T, Mathieu V, et al. (2013) A review of the current status of siRNA nanomedicines in the treatment of cancer. *Biomaterials* 34: 6429–6443.
2. Oh Y-K, Park TG (2009) siRNA delivery systems for cancer treatment. *Adv Drug Deliver Rev* 61: 850–862.
3. Fire A (1999) RNA-triggered gene silencing. *Trends Genet* 15: 358–363.
4. Fire A, Xu SQ, Montgomery MK, et al. (1998) Potent and specific genetic interference by double-stranded RNA in Caenorhabditis elegans. *Nature* 391: 806–811.
5. Aliabadi HM, Landry B, Sun C, et al. (2012) Supramolecular assemblies in functional siRNA delivery: where do we stand? *Biomaterials* 33: 2546–2569.
6. Guo P, Coban O, Snead NM, et al. (2010) Engineering RNA for targeted siRNA delivery and medical application. *Adv Drug Deliver Rev* 62: 650–666.
7. Sheikhi Mehrabadi F, Fischer W, Haag R (2012) Dendritic and lipid-based carriers for gene/siRNA delivery (a review). *Curr Opin Solid St M* 16: 310–322.
8. Gonzalez H, Hwang SJ, Davis ME (1999) New class of polymers for the delivery of macromolecular therapeutics. *Bioconjugate Chem* 10: 1068–1074.
9. Zhang S, Zhao B, Jiang H, et al. (2007) Cationic lipids and polymers mediated vectors for delivery of siRNA. *J Control Release* 123: 1–10.
10. Ballar ń-Gonz ález B, Ebbesen MF, Howard KA (2013) Polycation-based nanoparticles for RNAi-mediated cancer treatment. *Cancer Lett.*
11. Fischer D, Bieber T, Li Y, et al. (1999) A Novel Non-Viral Vector for DNA Delivery Based on Low Molecular Weight, Branched Polyethylenimine: Effect of Molecular Weight on Transfection Efficiency and Cytotoxicity. *Pharm Res* 16: 1273–1279.

12. Richards Grayson A, Doody A, Putnam D (2006) Biophysical and Structural Characterization of Polyethylenimine-Mediated siRNA Delivery in Vitro. *Pharm Res* 23: 1868–1876.
13. Wightman L, Kircheis R, Rössler V, et al. (2001) Different behavior of branched and linear polyethylenimine for gene delivery in vitro and in vivo. *J Gene Med* 3: 362–372.
14. Merkel OM, Beyerle A, Beckmann BM, et al. (2011) Polymer-related off-target effects in non-viral siRNA delivery. *Biomaterials* 32: 2388–2398.
15. Akhtar S, Benter I (2007) Toxicogenomics of non-viral drug delivery systems for RNAi: potential impact on siRNA-mediated gene silencing activity and specificity. *Adv Drug Deliver Rev* 59: 164–182.
16. Zuckerman JE, Choi CHJ, Han H, et al. (2012) Polycation-siRNA nanoparticles can disassemble at the kidney glomerular basement membrane. *PNAS* 109: 3137–3142.
17. Nel AE, Madler L, Velegol D, et al. (2009) Understanding biophysicochemical interactions at the nano-bio interface. *Nat Mater* 8: 543–557.
18. Albanese A, Tang PS, Chan WCW (2012) The effect of nanoparticle size, shape, and surface chemistry on biological systems. *Annu Rev Biomed Eng* 14: 1–16.
19. Lv H, Zhang S, Wang B, et al. (2006) Toxicity of cationic lipids and cationic polymers in gene delivery. *J Control Release* 114: 100–109.
20. He C, Hu Y, Yin L, et al. (2010) Effects of particle size and surface charge on cellular uptake and biodistribution of polymeric nanoparticles. *Biomaterials* 31: 3657–3666.
21. Zintchenko A, Philipp A, Dehshahri A, et al. (2008) Simple modifications of branched PEI lead to highly efficient siRNA carriers with low toxicity. *Bioconjugate Chem* 19: 1448-1455.
22. Pasche S, Vörös J, Griesser HJ, et al. (2005) Effects of Ionic Strength and Surface Charge on Protein Adsorption at PEGylated Surfaces. *J Phys Chem B* 109: 17545–17552.
23. Miteva M, Kirkbride KC, Kilchrist KV, et al. (2014) Tuning PEGylation of mixed micelles to overcome intracellular and systemic siRNA delivery barriers. *Biomaterials*.
24. Zhu C, Jung S, Luo S, et al. (2010) Biomaterials Co-delivery of siRNA and paclitaxel into cancer cells by biodegradable cationic micelles based on PDMAEMA – PCL – PDMAEMA triblock copolymers. *Biomaterials* 31: 2408–2416.
25. Kim D, Lee D, Jang YL, et al. (2012) Facial amphipathic deoxycholic acid-modified polyethyleneimine for efficient MMP-2 siRNA delivery in vascular smooth muscle cells. *Eur J Pharm Biopharm* 81: 14–23.
26. Hong J, Ku SH, Lee MS, et al. (2014) Cardiac RNAi therapy using RAGE siRNA/deoxycholic acid-modified polyethylenimine complexes for myocardial infarction. *Biomaterials* 35: 7562–7573.
27. Patel MM, Anchordoquy TJ (2005) Contribution of Hydrophobicity to Thermodynamics of Ligand-DNA Binding and DNA Collapse. *Biophys J* 88: 2089–2103.
28. Kim HJ, Miyata K, Nomoto T, et al. (2014) siRNA delivery from triblock copolymer micelles with spatially-ordered compartments of PEG shell, siRNA-loaded intermediate layer, and hydrophobic core. *Biomaterials* 35: 4548–4556.
29. Bartlett DW, Davis ME (2006) Insights into the kinetics of siRNA-mediated gene silencing from live-cell and live-animal bioluminescent imaging. *Nucleic Acids Res* 34: 322–333.
30. Matsumoto S, Christie RJ, Nishiyama N, et al. (2009) Environment-Responsive Block Copolymer Micelles with a Disulfide Cross-Linked Core for Enhanced siRNA Delivery. *Biomacromolecules* 10: 119–127.

31. Xia W, Wang P, Lin C, et al. (2012) Bioreducible polyethylenimine-delivered siRNA targeting human telomerase reverse transcriptase inhibits HepG2 cell growth in vitro and in vivo. *J Control Release* 157: 427–436.
32. Nelson CE, Kintzing JR, Hanna A, et al. (2013) Balancing cationic and hydrophobic content of PEGylated siRNA polyplexes enhances endosome escape, stability, blood circulation time, and bioactivity in vivo. *ACS nano* 7: 8870–8880.
33. Petros Ra, DeSimone JM (2010) Strategies in the design of nanoparticles for therapeutic applications. *Nat Rev Drug Discov* 9: 615–627.
34. Maeda H, Wu J, Sawa T, et al. (2000) Tumor vascular permeability and the EPR effect in macromolecular therapeutics: a review. *J Control Release* 65: 271–284.
35. Holzerny P, Ajdini B, Heusermann W, et al. (2012) Biophysical properties of chitosan/siRNA polyplexes: profiling the polymer/siRNA interactions and bioactivity. *J Control Release* 157: 297–304.
36. Guo G, Zhou L, Chen Z, et al. (2013) Alkane-modified low-molecular-weight polyethylenimine with enhanced gene silencing for siRNA delivery. *Int J Pharm* 450: 44–52.
37. Canton I, Battaglia G (2012) Endocytosis at the nanoscale. *Chem Soc Rev*.
38. Noguchi A, Furuno T, Kawaura C, et al. (1998) Membrane fusion plays an important role in gene transfection mediated by cationic liposomes. *FEBS Lett* 433: 169–173.
39. Cevc G, Richardsen H (1999) Lipid vesicles and membrane fusion. *Adv Drug Deliver Rev* 38: 207–232.
40. Akinc A, Thomas M, Klibanov AM, et al. (2005) Exploring polyethylenimine-mediated DNA transfection and the proton sponge hypothesis. *J Gene Med* 7: 657–663.
41. Pack DW, Hoffman AS, Pun S, et al. (2005) Design and development of polymers for gene delivery. *Nat Rev Drug Discov* 4: 581–593.
42. Kurtulus I, Yilmaz G, Ucuncu M, et al. (2014) A new proton sponge polymer synthesized by RAFT polymerization for intracellular delivery of biotherapeutics. *Polymer Chem* 5: 1593–1604.
43. Richard I, Thibault M, De Crescenzo G, et al. (2013) Ionization Behavior of Chitosan and Chitosan–DNA Polyplexes Indicate That Chitosan Has a Similar Capability to Induce a Proton-Sponge Effect as PEI. *Biomacromolecules* 14: 1732–1740.

AIMS Press